Chemical Engineering Communications
Publication details, including instructions for authors and subscription information:
http://www.informaworld.com/smpp/title~content=t713454788

UPPER BOUND ON THE STRESS-INDUCED MIGRATION EFFECT IN LAMINAR FALLING FILM FLOWS OF DILUTE POLYMER SOLUTIONS

A. Dutta[a]; R. A. Mashelkar[a]
[a] Polymer Science and Engineering Group Chemical Engineering Division National Chemical Laboratory, Pune, India

To cite this Article Dutta, A. and Mashelkar, R. A.(1985) 'UPPER BOUND ON THE STRESS-INDUCED MIGRATION EFFECT IN LAMINAR FALLING FILM FLOWS OF DILUTE POLYMER SOLUTIONS', Chemical Engineering Communications, 39: 1, 277 — 296
To link to this Article: DOI: 10.1080/00986448508911677
URL: http://dx.doi.org/10.1080/00986448508911677

Chem. Eng. Commun. Vol. 39 pp. 277–296
0098-6445/85/3906-0277$20.00/0

Printed in the United States of America

UPPER BOUND ON THE STRESS-INDUCED MIGRATION EFFECT IN LAMINAR FALLING FILM FLOWS OF DILUTE POLYMER SOLUTIONS†

A. DUTTA and R.A. MASHELKAR

Polymer Science and Engineering Group
Chemical Engineering Division
National Chemical Laboratory
Pune 411 008, India

(*Received July 19, 1984; in final form April 9, 1985*)

The role of stress-induced migration in falling film flows of dilute polymer solutions is analysed for the limiting case of fully developed concentration field (FDCF). This theoretically derived asymptote is anticipated to serve as an upper bound on the migration effect and our predictions are shown to be consistent with available experimental observations. However, considerable difference between the FDCF asymptote and the experimental data suggests lack of fully developed conditions in most experiments and hence implies the possibility of flow length dependence, a factor hitherto not considered. Finally, a simple approach based on a two-phase model is developed in order to estimate the order of magnitude of film thickness variation that develops along the film length as migration progresses.
KEYWORDS Stress induced migration Film flow Polymer solution

INTRODUCTION

In laminar falling film flows of dilute polymer solutions, it has been observed that the experimentally determined flow rate is considerably greater (as high as 300%) than that predicted by the conventional non-Newtonian theory [1–4]. Phenomenologically, this flow enhacement can be interpreted as being due to effective wall slip caused by the formation of a low-viscosity polymer depleted zone adjacent to the rigid surface [2–5]. As indicated by Mashelkar and Dutta [6], such slip effects can play a prominent role in heat and mass transfer operations involving film flows of polymer solutions. Indeed, they show that these effects could explain several anomalous observations, which were hitherto unexplained. Although many hypotheses, based on thermodynamical arguments [7–8] or kinetic theory approaches [9–10] have highlighted the aspects of macromolecular migration, the precise mechanism by which such migration of the polymer molecules away from the high deformation-rate wall regions occurs is still not clearly established. Besides, several other mechanistic interpretations based

† NCL Communication No. 3589
Submitted for publication by J. J. Ulbrecht.

primarily on pure fluid mechanical arguments have also been suggested and salient features of these hypotheses were summarized in an earlier publication [12].

Thermodynamical reasoning, representing one of the schools of thought, suggests that the macromolecular migration phenomenon is essentially the manifestation of the free energy equilibration process necessitated by the non-uniform nature of the velocity field [7–9]. In particular, it is argued that in any flow process with spatially varying velocity gradients, the molecular orientation and extension and consequently the free energy level varies with the location within the fluid. Compensating concentration gradients are therefore induced in order to allow the free energy to be position independent. The resultant effect is that the polymer molecules tend to move towards region of lower deformation rates. As a result, a polymer-depleted low-viscosity layer is formed (at the high deformation rate regions) near the rigid walls over which the bulk of the high-viscosity liquid core appears to 'slip' through.

An unanswered question concerning this hypothesis pertains to the order of flow times (or lengths) necessary for observable migration effect. Metzner *et al.* [9] suggest that since the migration occurs actually by the very slow process of macromolecular diffusion, adequate diffusion time must be available to the flowing liquid for appreciable development of the non-uniform concentration field. Indeed, for capillary flows, numerical calculations by Tirrell and Malone [10] and Cohen and Metzner [13, 14] predict that very large lengths (up to 5000 diameters) are required in order to attain fully developed concentration fields. These analyses, however, either neglected the strong viscosity-concentration coupling or involved several simplifying assumptions and hence the above results may be somewhat exaggerated. For a more realistic analysis, the developing flow problem needs to be solved more rigorously incorporating the viscosity concentration coupling.

Janssen [11], on the other hand, speculated that owing to the severe coupling between the viscosity and the polymer concentration a 'runaway' mechanism will be operative and the concentration redistribution will be complete within a relatively short time. In support of this notion, he referred to the observation of constant film thickness being attained within a short distance for falling film flows of polymer solutions. Janssen's analytical development, based on a Hookean dumbell model valid for very dilute solutions, however, does not concern with this instability postulate but demonstrates the significance of viscosity-concentration coupling on the migration process under fully developed conditions. In an earlier publication [15], we have extended Janssen's analysis and compared the theoretical predictions with Popadic's data (1) for film flow of Carbopol solutions. Significant differences were observed between theory and experiments thereby casting some doubt on the instability mechanism invoked by Janssen. Nevertheless, the analytical results served as an upper bound on the migration effect. Apart from being applicable to very dilute polymer solutions only, Janssen's approach neglects the opposing influence of Fickean diffusion due to concentration difference and hence, here too, the theoretical prediction of flow enhancement are likely to be somewhat exaggerated.

In view of the above, it appears that the uncertainty regarding the exact nature of concentration (and subsequently velocity) field development needs to be resolved by undertaking a rigorous and detailed analysis of the problem. However, prior to initiating such a complex and involved effort, we deemed it appropriate to investigate the asymptotic stage of fully developed concentration field (FDCF) since this should provide an upper bound on the migration effect. Such an approach has successfully been applied to capillary flows of polymer solutions [12] and in the present work we extend this approach to an equally important problem of falling films. In doing so we develop a detailed analysis of the asymptotic case of full development. Following this, the available experimental data are compared with the FDCF aymptote in order to assess the state of development attained in these experiments. Such information should then provide guidelines for further more carefully controlled experimentation. Finally, we shall consider the implication of the FDCF asymptote and, in light of the present findings, discuss an approach, based on a simple two-phase model, that permits estimation of the order of film thickness variation caused by polymer migration.

MATHEMATICAL FORMULATION

We consider the steady laminar film flow of a polymer solution as shown schematically in Figure 1(a). Initially (at $x = 0$) the polymer concentration, c_i, is uniform and as it flows down the inclined rigid surface polymer migration occurs. A polymer depleted layer develops near the wall and finally a fully developed concentration profile is achieved. At full development, both the concentration and the velocity fields are independent of the flow length, x, and therefore the transverse velocity, V_y, vanishes. Besides, since migration is effected by a very slow diffusive process the axial flux can be taken to be negligible as compared to the corresponding transverse flux. Under these conditions, the momentum and the diffusion equations simplify to

$$\tau_{xy} = \tau_w \xi \tag{1}$$

and

$$J_y = 0 \tag{2}$$

where $\xi = y/\delta$, y is the transverse distance, δ the film thickness, and $\tau_w = \rho g \delta \cos \beta$ the wall shear stress. The transverse diffusion flux, J_y, comprises two components viz. the usual Fickean component and the component arising out of spatial entropy variation. Cohen [14], shows that if $f = f(\lambda, \dot{\gamma})$ represents a dimensionless chemical potential function the transverse flux can be written as

$$J_y = -\frac{D_0 c_i}{\delta}\left[\phi \frac{d\theta}{d\xi} + \theta \frac{df}{d\xi}\right] \tag{3}$$

where $\theta = c/c_i$ is the dimensionless concentration, $\lambda = \lambda(c, \dot{\gamma})$ is the fluid relaxation time, D_0 the binary diffusion coefficient, $\phi = \phi(c)$ is a correction factor that accounts for the concentration dependence of diffusivity, and $\dot{\gamma} = \dot{\gamma}(c, y)$ is the

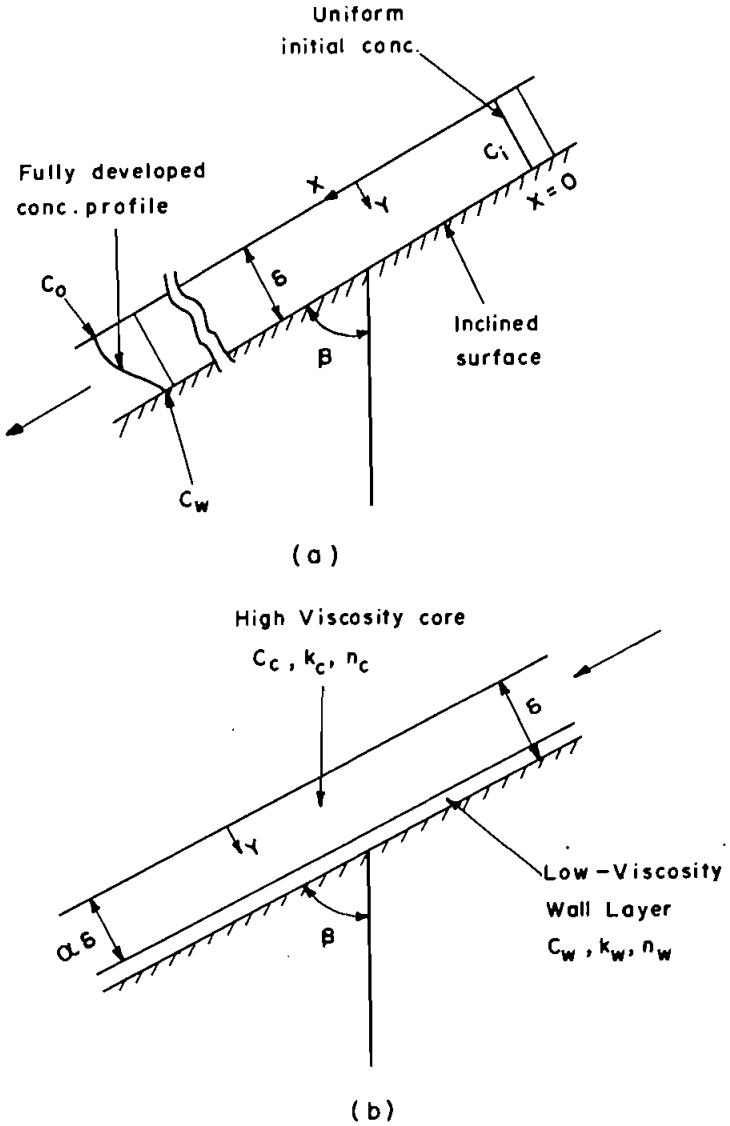

FIGURE 1 Schematic representation of (a) falling film flow and (b) two-phase model.

shear rate given as

$$\dot{\gamma} = -\frac{V}{\delta}\frac{d\psi}{d\xi} = \frac{\tau_w \xi}{\eta} \tag{4}$$

where $\eta = \eta(c, \dot{\gamma})$ is the shear viscosity and $\psi = V_x/V$ is the dimensionless longitudinal velocity, V being the mean velocity. Since the potential function f depends on λ which in turn depends on the concentration, c, straightforward substitution of Eq. (3) in Eq. (2) yields an implicit equation in dc/dr. By

expressing df/dr in terms of appropriate partial derivatives, the following explicit expression for the dimensionless concentration gradient can be obtained [12].

$$\frac{d\theta}{d\xi} = -\frac{\theta\left(\frac{\partial f}{\partial \lambda}\frac{\partial \lambda}{\partial \dot{\gamma}} + \frac{\partial f}{\partial \dot{\gamma}}\right)\frac{\partial \dot{\gamma}}{\partial \xi}}{\phi + \theta\frac{\partial f}{\partial \lambda}\frac{\partial \lambda}{\partial \theta} + \theta\left(\frac{\partial f}{\partial \lambda}\frac{\partial \lambda}{\partial \dot{\gamma}} + \frac{\partial f}{\partial \dot{\gamma}}\right)\frac{\partial \dot{\gamma}}{\partial \theta}} \tag{5}$$

Although no boundary condition can be specified for the concentration profile obtained as the solution to Eq. (5), the latter equation must satisfy the following mass balance relationship

$$\int_0^1 \psi\theta \, d\xi = \int_0^1 \psi \, d\xi \tag{6}$$

Thus in order to obtain the fully developed velocity and concentration profiles Eqs. (4) and (5) must be simultaneously solved subject to the conditions $\psi(1) = 0$ and that given by Eq. (6). In order to do so, an explicit expression for the potential function f is necessary. For dilute solutions, if the polymer molecule is approximated as linear dumbells, f can be expressed as [14, 16]

$$f = (\lambda\dot{\gamma})^2 - \tfrac{1}{2}\ln(1 + 2(\lambda\dot{\gamma})^2) \tag{7}$$

where the relaxation time λ can be determined from the following relationship

$$\lambda = N_1/2\tau_{xy}\dot{\gamma} \tag{8}$$

where N_1 is the primary normal stress difference.

The above formulation is of general nature and is applicable for any given description of the rheological behaviour. An interesting conclusion that emerges from the analysis is that for any given wall shear stress (τ_w) and initial polymer concentration (c_i), the concentration profile, $\theta(\xi)$, is independent of the film thickness. This is obvious since all the partial derivatives in Eq. (5) are independent of δ. In addition, as the volumetric flow rate per unit width (q) is

$$q = \tau_w\delta^2 \int_0^1 \int_\xi^1 \frac{\xi^* \, d\xi^*}{\eta(c, \dot{\gamma}^*)} \, d\xi \tag{9}$$

where $\dot{\gamma}^* = \dot{\gamma}(c, \xi^*)$, it is evident that the apparent wall shear rate, $3q/\delta^2$ is a function of τ_w and c_i only. Thus, under fully developed conditions, the flow curve for a given polymer will be a unique one, representing the maximum possible flow enhancement due to migration.

For most polymer solutions, within the shear rate ranges of practical interest, the shear rate dependence of both the shear viscosity and the primary normal stress difference can be adequately represented by a power-law behaviour written as follows

$$\eta = K(c)\dot{\gamma}^{n(c)-1}, \qquad N_1 = A(c)\dot{\gamma}^{p(c)} \tag{10}$$

In order to solve Eq. (5), the concentration dependence of the rheological

parameters (K, n, A, and p) needs to be known. These are determined experimentally and usually these also follow a power-law behaviour with reference to concentrations and can be represented as

$$K = a_1 c^{b_1}, \qquad n = a_2 c^{b_2}, \qquad A = a_3 c^{b_3}, \quad \text{and} \quad p = a_4 c^{b_4} \tag{11}$$

where a's and b's are constants. In the following, we obtain the detailed concentration and velocity fields assuming the above power-law relationships for different rheological parameters and material functions.

A fourth-order Runge–Kutta technique was employed to numerically solve the governing equations. Since the free-surface concentration, c_0, is not known *a priori* a shooting type procedure was necessary and an initial guess of c_0 was adjusted until the mass balance condition represented by Eq. (6) was satisfied.

MATERIAL PARAMETERS

The objective of the numerical calculations is to obtain theoretical predictions for those conditions of falling film flows under which experimental observations of flow enhancement were made. Although several such observations have been reported [1–4], none of them contain the complete rheological information necessary for undertaking the calculations. Carreau *et al.* [3] have conducted an extensive experimental study of the anomalous flow effects in falling film flows of aqueous polyacrylamide (Separan MG-700, Mol. wt. $\sim 6 \times 10^6$ [17]) and carboxymethyl cellulose solutions. Along with the film flow data, they have also presented the viscosity-shear rate data for different polymer concentration. Within the power law region (shear rate $> 1\ \text{sec}^{-1}$) of the viscosity curves for the Separan solutions, the following constants could be obtained

$$\begin{aligned} a_1 &= 83.132 \text{ dynes sec}^n/\text{cm}^2, \qquad b_1 = 1.297 \\ a_2 &= 0.3101 \text{ dynes sec}^p/\text{cm}^2, \qquad b_2 = -0.1466 \end{aligned} \tag{12}$$

where the polymer concentration c is in weight percent. Unfortunately, however, no data regarding the primary normal stress difference was reported. Similar lack of normal stress data is also evident in other data sources too.

In the absence of experimental normal stress data, we sought to generate this information from shear viscosity data using the procedure suggested by Abdel-Khalik *et al.* [18] and Wagner [19]. Both these methods, however, predict similar dependence of shear and normal stress on the shear rate ($p = n$) whereas for most polymer solutions in the range of shear rates of interest to us, we find that $p > n$. Further, when $p = n$, the free energy function becomes independent of shear rate (see eq. (7)). This is presumably an artifact of these proposed methods.

An alternative semi-empirical procedure was thus devised in order to generate the normal stress information from shear viscosity data. From molecular theory of dilute polymer solutions, an expression for the relaxation time analogous to that suggested by Peterlin [16] can be written as

$$\lambda = \frac{\eta_s [\eta] M}{RT} \tag{13}$$

where η_s is the solvent viscosity, $[\eta]$ the shear dependent intrinsic viscosity [20], M the polymer molecular weight, R the gas constant, and T the absolute temperature. Following Eq. (13), for our purpose it is convenient to hypothesize the following expression for λ

$$\lambda = \frac{100M\eta}{\rho cRT} \tag{14}$$

where ρ is the solution density, c the concentration in weight percent, and η_s is taken to be negligible as compared to the shear viscosity, η. Combining Eqs. (8) and (14), the normal stress can be written as

$$N_1 = \frac{200M}{\rho cRT}\tau_{xy}^2 \tag{15}$$

If the shear stress (τ_{xy}) follows a power law relationship as represented by Eqs. (10), then from Eqs. (11) and (15) we get

$$a_3 = \frac{200Ma_1^2}{\rho RT}, \qquad b_3 = 2b_1 - 1, \qquad a_4 = 2a_2, \qquad b_4 = b_2 \tag{16}$$

For the Separan solutions used by Carreau *et al.* this gives

$$a_3 = 337.64 \text{ dynes sec}^p/\text{cm}^2; \qquad b_3 = 1.594$$
$$a_4 = 0.6202, \qquad b_4 = -0.1466 \tag{17}$$

It must be emphasized that Eq. (14) is semi-empirical in nature and thus before using it for the numerical calculations we have compared the normal stresses predicated by Eq. (15) with the experimental data for several polyacrylamide solutions of different molecular weights. Such comparisons are presented in Table I and Figures 2 and 3 for aqueous solutions of laboratory prepared sample

TABLE I

Comparison between calculated and measured normal stresses for 2% polyacrylamide solution

Shear rate (sec^{-1})	Shear stress (dynes/cm^2)	Normal stress (dynes/cm^2) Calculated	Measured [21]
0.6	70	104.5	90
1.0	85	154.5	150
1.6	100	214.0	220
2.6	140	419.0	320
4.0	160	547.0	440
6.0	180	693.0	600
10	210	943.0	750
16.0	240	1230.0	930
25.0	280	1680.0	1150
60.0	370	2930.0	2000
90.0	440	4140.0	2800
140.0	500	5340.0	3150
210.0	590	7440.0	4500
350.0	630	8490.0	8000
850.0	900	17320.0	10500

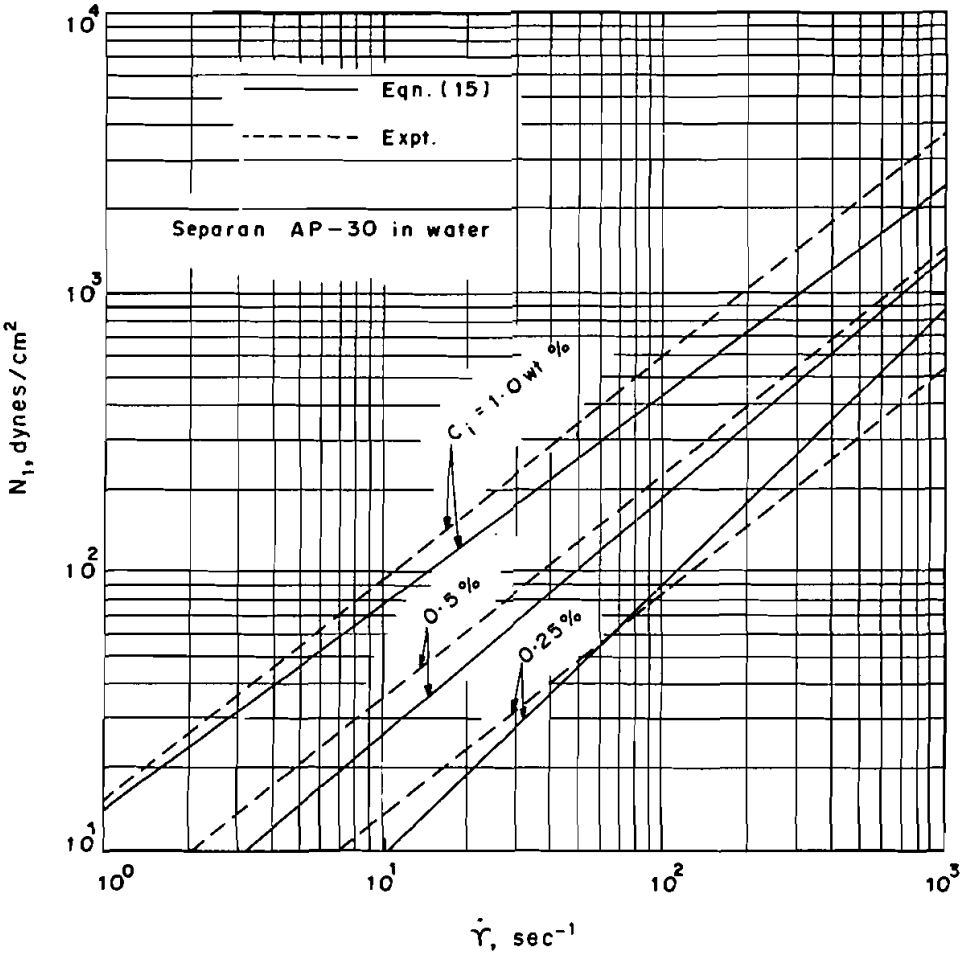

FIGURE 2 Comparison between predicted and measured [14] normal stress difference for Separan AP-30 solutions in water.

($M = 5.3 \times 10^6$ [21]), Separan AP-30 ($M = 1.75 \times 10^6$ [14]), and MG-273 ($M = 6 \times 10^6$ [22]) respectively. Reasonably, good agreement between Eq. (15) and experimental data is evident. Since the molecular weight and the concentration range for the MG-700 solutions used by Carreau *et al.* are similar to those for the above test solutions, we expect the normal stress difference predicted by Eq. (15) to be reasonably close to the actual values. The calculations, to be presented in the following, therefore were made using the constant values given by Eqs. (12) and (17).

Apart from rheological information, knowledge about the concentration dependence of the diffusion coefficient (D) is also necessary. For dilute polymer solutions, D typically varies as follows [23].

$$D = D_0\phi \quad \text{where} \quad \phi = 1 + k_D c \tag{18}$$

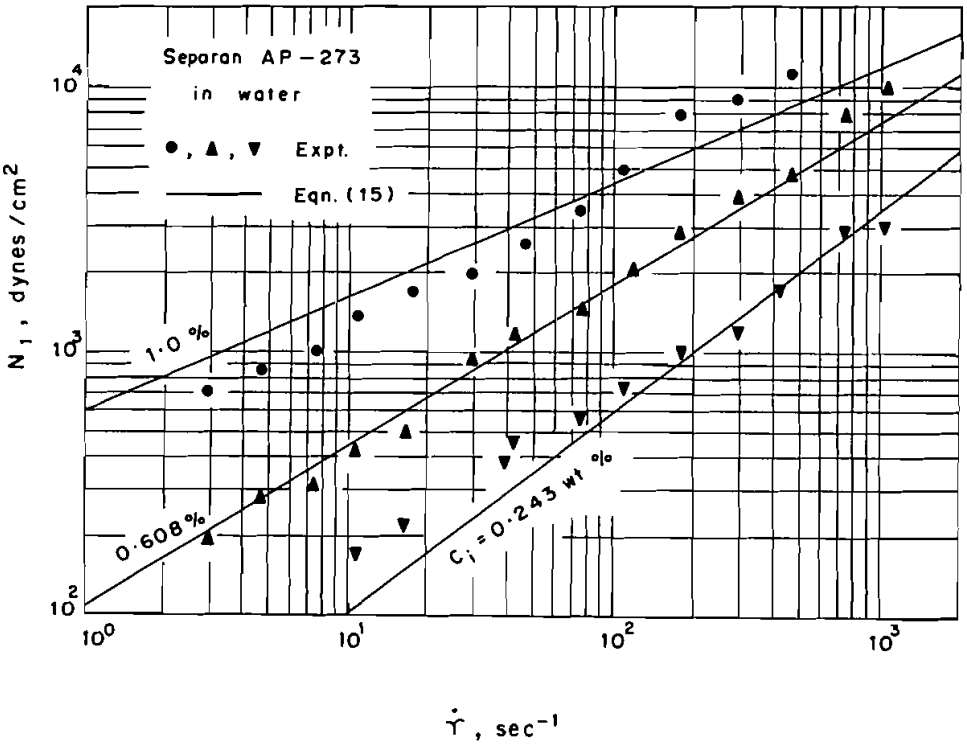

FIGURE 3 Comparison between predicted and measured [22] normal stress difference for aqueous Separan AP-273 solutions.

Scholtan [24] has experimentally confirmed this linear behaviour for aqueous polyacrylamide solutions and found that k_D is a strongly increasing function of molecular weight particularly at high values. For $M = 6 \times 10^6$, the experimental results can be extrapolated to estimate k_D to be roughly 2.21 and this value is used to describe the function ϕ for Separan MG-700 solutions. Since this k_D value is only an estimate, the sensitivity of the numerical results to any change in k_D was investigated. It was found that even for $\pm 50\%$ variation in k_D, the corresponding changes in concentration and flow enhancement ratios are about $\pm 3\%$ and $\pm 7\%$, respectively. Thus, even though $k_D = 2.21$ is only approximate, the subsequent numerical results are not expected to be altered significantly when a more exact value is used.

NUMERICAL RESULTS

Figure 4 illustrates typical fully developed concentration and velocity profiles for a given shear stress and initial polymer concentration for falling film flow of aqueous Separan MG-700 solutions. Owing to migration, the region adjacent to the rigid (inclined) surface sees concentration depletion while a corresponding

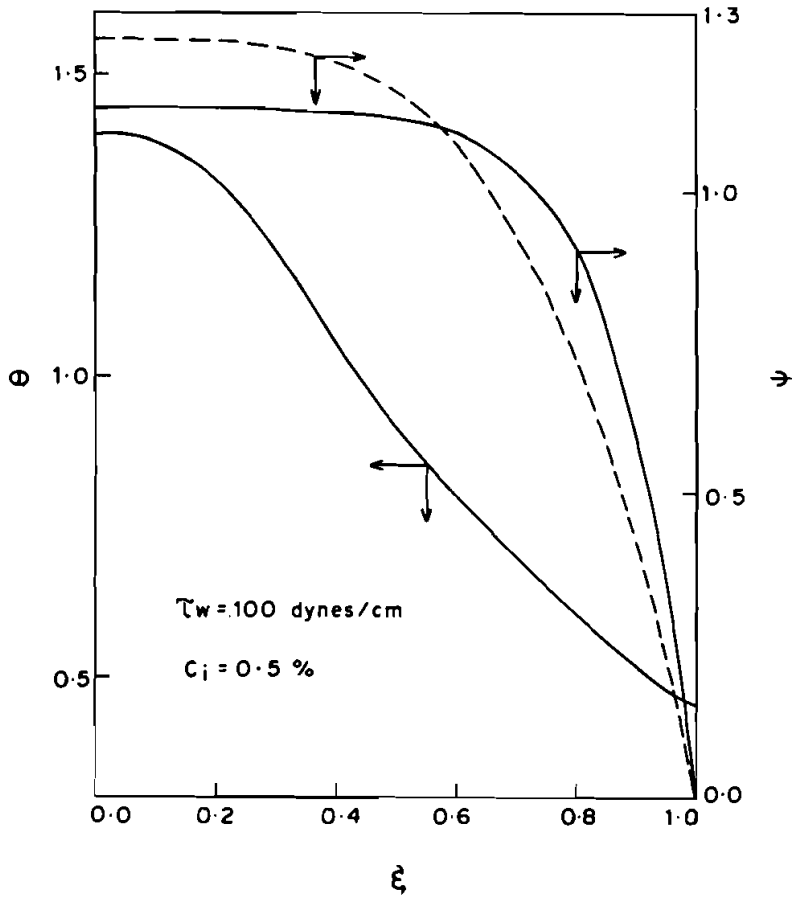

FIGURE 4 Typical fully developed concentration and velocity profiles for film flow of Separan MG-700 solution. The broken line represents the velocity profile in the absence of migration.

concentration increase occurs near the free surface of the film. This leads to a highly non-uniform concentration distribution as shown in Figure 4. As a consequence of this concentration field, the viscosities are lower near the rigid surface and the velocities are higher, whereas the reverse holds true near the free surface. The net effect therefore is a tendency for the velocity field to become more uniform across the film. From Figure 4 is is seen that, in comparison to the velocity profile in the absence of migration (no-slip case), migration results in a much blunter profile accompanied by a marked increase in the wall shear rate.

Table II, which summarizes the numerical result, indicate the controlling influences of both the applied shear stress, τ_w, and the solution concentration, c_i. As in capillary flows [12], for a given c_i the extent of separation $\Delta c = (c_0 - c_w)/c_i$ increases with τ_w whereas for a given τ_w, Δc diminishes as the solution gets more concentrated. This behavior is caused by the opposing influences of concentration on the relaxation time and the shear rate which jointly controls the potential function, f—the driving force behind stress-induced migration.

TABLE II

Summary of numerical results for aqueous Separan MG-700 solutions

τ_w (dynes/cm^2)	c_0/c_i	c_w†$/c_i$	q/q_{ns}	q/δ^2 (sec^{-1})	V_s/V	$\psi(0)$	$\left.\frac{d\psi}{d\xi}\right\|_{\xi=1}$
				$c_i = 0.5$ wt.%			
70	1.2696	0.5338	4.482	7.536	0.777	1.151	7.447
80	1.3142	0.4972	5.139	12.750	0.805	1.148	7.620
90	1.3600	0.4652	5.775	20.320	0.827	1.144	7.795
100	1.4004	0.4346	6.475	30.970	0.846	1.141	7.978
121	1.4806	0.3790	7.910	65.510	0.874	1.134	8.436
				$c_i = 0.6$ wt.%			
70	1.1965	0.6157	3.459	2.988	0.711	1.159	7.118
87.5	1.2617	0.5623	4.218	7.110	0.763	1.153	7.317
95	1.2878	0.5425	4.539	9.777	0.780	1.151	7.387
100	1.3037	0.5288	4.786	12.020	0.791	1.150	7.442
115	1.3547	0.4950	5.419	20.080	0.815	1.146	7.591
130	1.4000	0.4643	6.063	33.600	0.835	1.144	7.743
150	1.4583	0.4280	6.914	58.800	0.855	1.141	7.962
				$c_i = 0.7$ wt.%			
100	1.2369	0.5943	3.892	5.540	0.743	1.156	7.195
130.5	1.3196	0.5350	4.855	15.610	0.794	1.151	7.404
138	1.3399	0.5217	5.103	19.590	0.804	1.149	7.451
150	1.3687	0.5049	5.412	26.660	0.815	1.148	7.524
158	1.3870	0.4924	5.673	32.740	0.824	1.147	7.576
164	1.4020	0.4850	5.800	37.530	0.828	1.146	7.610

† c_w is the wall concentration.

As mentioned earlier, the phenomenon of stress-induced migration is manifested as a marked increase in volumetric flow rate. Figure 5(a) shows the calculated flow enhancement ratio q/q_{ns} (where q_{ns} is the volumetric flow rate per unit width in the absence of migration) as a function of τ_w for three different concentrations. Functional dependence of this ratio on τ_w and c_i are analogous to that of Δc as discussed above. Note that these are qualitatively similar (see Figure 5b) to the shear stress and solution concentration dependence observed experimentally by Carreau *et al.* [3]. As discussed later, a quantitative agreement between the FDCF predictions and the experimental data is anticipated only if fully developed conditions are ensured during the flow measurements. Regarding the drastic increase in volumetric rate, it is seen from Figure 5(a) that depending on the particular combination of τ_w and c_i, the flow rate can be anywhere between 200 to 600% higher than the no-slip value. These are major slip effects and, as discussed by Mashelkar and Dutta [6], neglecting them can lead to apparently anomalous behaviours in interpretation of heat and mass transfer processes in falling film flows of polymer solutions. For a more direct estimation of slip flow

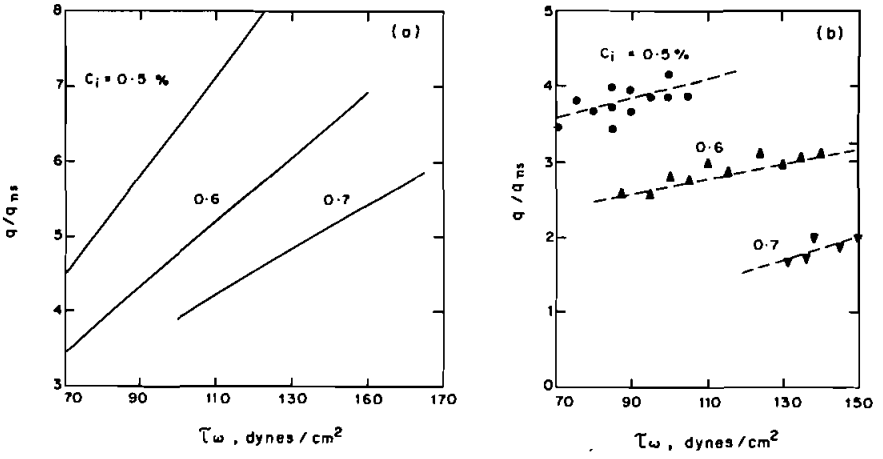

FIGURE 5 Flow enhancement ratio as a function of wall shear stress for aqueous Separan MG-700 solutions. (a) fully developed calculations (b) experimental data [3]. Broken line indicates the trend of experimental observations.

contribution to total flow, the following expression can be made use of

$$v_s/V = 1 - q_{ns}/q \tag{19}$$

where v_s is the effective slip velocity. Numerical results suggest that in film flows of the Separan MG-700 solutions considered in this work, this contribution can be as high as 70 to 90% (see Table II). Such large slip flow contribution was also shown to be likely for a similar flow configuration in free coating of polymer solutions (25).

COMPARISON WITH EXPERIMENTAL DATA

In order to assess the state of development of the concentration (and hence velocity) fields, we compare the theoretical results with experimental data reported by Carreau *et al.* [3] for falling film flows of aqueous Separan MG-700 solutions. Flow curves for different polymer concentrations are shown in Figures 6 to 8. In all the cases, the measured flow rate is higher than the no-slip prediction but considerably lower than the FDCF asymptote. That is the data are bounded by the no-slip calculations and the fully developed prediction, with the latter serving as the upper bound on the migration effect. Note that for a specified τ_w and c_i, this asymptotic flow curve is unique and does not depend on any other flow variables such as film thickness, (δ) and the angle of inclination (β). In a separate publication [12], similar observations were reported by us for capillary flows of aqueous Separan AP-30 solutions.

Comparisons between theory and experiments, presented in Figures 6 to 8 suggest that in all the cases the measured flow rate is considerably less than the FDCF asymptotic value but greater than the no-slip prediction. Furthermore, this

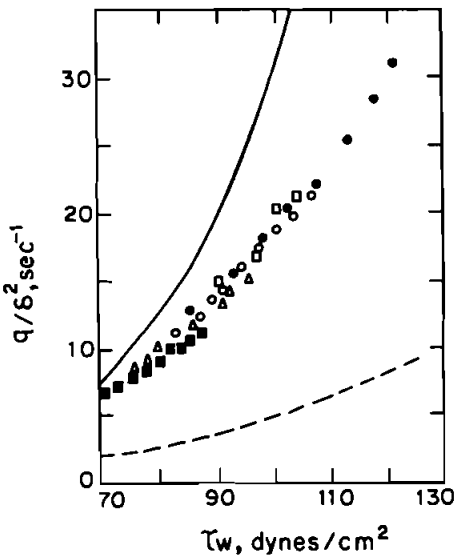

FIGURE 6 Flow curves for 0.5% Separan MG-700 solution. Calculated: [——] FDCF asymptote, [----] no-slip calculation. Experimental (3): $\beta = 85°$ (■), 82.5° (△), 80°(○), 77.5° (□) 75° (●).

discrepancy between FDCF asymptote and experimental data becomes more pronounced as τ_w increases. A plausible explanation of this behaviour is that the experimental measurements pertain to the developing flow regime and not the fully developed conditions. In their experiments, Carreau *et al.* specify a flow length of 100 cm. The significant difference between their experimental measurement and the FDCF asymptote implies that this length, perhaps, is not sufficient for the flow to become fully developed. Besides, for a constant flow length, it is expected that with an increase in τ_w, the full development will be even further delayed. Thus the discrepancy between FDCF prediction and the experimental measurements will be even more prominent. It then follows that if experiments are conducted in the developing flow regime, the results will depend on the flow length and unless the length dependence is accounted for, the correlations based on the data generated will be of little value.

Presently, no guidelines are available for determining the order of flow length necessary for full development of the migration phenomenon. Apart from developing a rigorous theoretical treatment of the developing flow problem, an alternative approach would be to experimentally investigate the length dependence of the anomalous flow effects in falling film flows of polymer solutions. The present theoretical development suggests that beyond a certain flow length, no further migration is possible and the flow enhancement ratio will reach 'saturation' and will cease to increase with any further increase in the shear stress.

In the light of the preceding discussion, it appears that very long flow length will be necessary for completion of flow development and hence attainment of a constant film thickness. Experimental observations, however, suggest that a

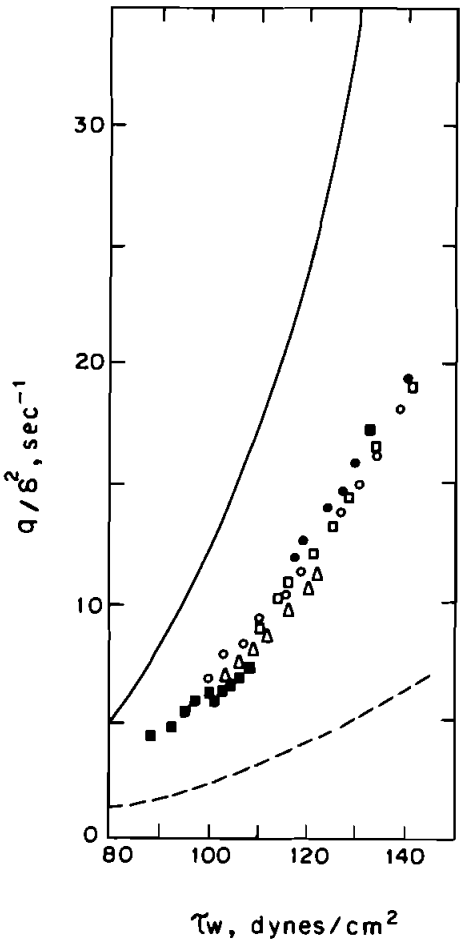

FIGURE 7 Flow curves for 0.6% Separan MG-700 solution. Legend is the same as in Figure 6.

constant film thickness appears to be attained within a relatively short distance for falling film flows [3]. The reason for this apparent discrepancy is not clear at the moment. However, some idea regarding the film thickness variation during the process of development can be obtained from an approximate phenomenological analysis of the problem. In the following section we will present such an analysis.

FILM THICKNESS VARIATION: A PHENOMENOLOGICAL ANALYSIS

We consider an idealized fully developed situation (see Figure 1(b)) where two distinct layers have been formed due to polymer migration away from the wall. Close to the wall there is a low viscosity layer over which the bulk of the polymer solution is flowing. If the layer thickness is $(1-\alpha)$ times the film thickness (δ) and

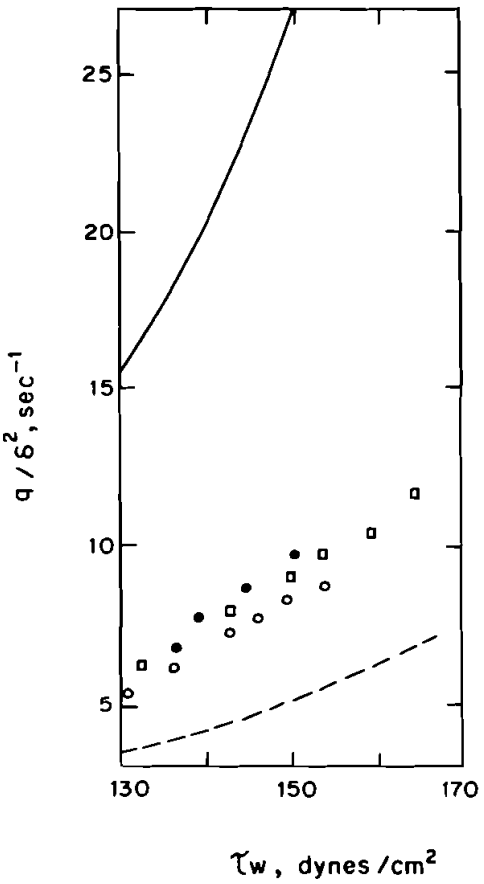

FIGURE 8 Flow curves for 0.7% Separan MG-700 solution. Legend is the same as in Figure 6.

both the phases follow powerlaw behaviour, then the volumetric flow rate per unit width can be expressed as

$$q = \frac{n_w}{2n_w+1}\left(\frac{\tau_w}{K_w}\right)^{1/n_w}\delta^2(1-\alpha^{2+1/n_w}) + \frac{n_c}{2n_c+1}\left(\frac{\tau_w}{K_c}\right)^{1/n_c}\delta^2\alpha^{2+1/n_c} \tag{20}$$

If q_{ns} is the flowrate in the absence of wallslip ($\alpha = 1$), the flow enhancement ratio becomes

$$\frac{q}{q_{ns}} = \alpha^{2+1/n_c} + \frac{2n_c+1}{2n_w+1}\cdot\frac{n_w}{n_c}\left(\frac{\tau_w}{K_w}\right)^{1/n_w}\left(\frac{K_c}{\tau_w}\right)^{1/n_c}(1-\alpha^{2+1/n_w}) \tag{21}$$

As the liquid film flows down the inclined plane, the initial part of it essentially represents a no-slip flow whereas after a certain length fully developed conditions are achieved. Since the flowrate will remain constant during this developing process, the ratio of downstream and upstream film thicknesses will be calculated

as follows

$$\frac{\delta}{\delta_{ns}} = \left[\frac{\dfrac{n_c}{2n_c+1}(\tau_w/k_c)^{1/n_c}}{\dfrac{n_w}{2n_w+1}\left(\dfrac{\tau_w}{K_w}\right)^{1/n_w}(1-\alpha^{2+1/n_w}) + \dfrac{n_c}{2n_c+1}\left(\dfrac{\tau_w}{K_c}\right)^{1/n_c}\alpha^{2+1/n_c}} \right]^{1/2} \tag{22}$$

For a given wall-layer concentration, c_w, the polymer concentration in the core layer (c_c) can be obtained from a mass balance equation which is

$$c_c = c_i + \frac{q_w}{q_c}(c_i - c_w) \tag{23}$$

Here c_i is the initial concentration and q_w and q_c are the volumetric flowrates in the wall and core layers, respectively. Equation (22) suggests that compared to the amount of flow enhancement the corresponding change in film thickness will be relatively small for typical (pseudoplastic) polymer solutions. For obtaining δ/δ_{ns}, however, an iterative procedure is necessary since the powerlaw constants K_c and n_c depends on the core concentration c_c (see Eq. (23)) not known *a priori*. As an example, let us consider the experimental data point (3) where $\tau_w = 87.5$ dynes/cm^2, $c_i = 0.6\%$ (aqueous Separan MG-700 solution), $q/q_{ns} = 2.598$. An iterative procedure suggests that $\alpha \sim 0.874$ and $c_c \sim 0.613$ for $c_w \sim 0.4$ as estimated by Carreau *et al.* [3]. Equation (27) then predicts $\delta/\delta_{ns} \sim 0.62$. Thus it is evident that even if the flow enhancement is of the order of 160%, the corresponding variation in film thickness is only about 38%. It is not clear to us as to whether a systematic investigation of such changes in film thickness over the entrie flow length has been attempted, but it would be decidedly desirable to do so.

Undoubtedly, the above model presents a simplistic view of the actual flow situation. Instead of a marked separation of two distinct layers, a gradual depletion of the polymer near the wall is more realistic (see Figure 4). Nevertheless, this simple model calculation does provide some interesting clues. In particular it suggests that film thickness variation owing to polymer migration will be relatively small as compared to the magnitude of flow enhancement. A detailed and careful study regarding the uniformity of film thickness along the flow length would indeed be fruitful in resolving as to whether stress-induced polymer migration proceeds via a slow diffusive process [9, 10, 13] or a fast 'runaway' mechanism [11]. Alternatively, it is also quite plausible that the high deformation rates prevailing in the hydrodynamic entrance region are adquate to set up the fully developed fields within a *relatively short flow length*. Future work in these directions will be decidedly rewarding in developing a better understanding of anomalous flow effects in laminar falling film flows of polymer solutions.

IMPLICATIONS IN MASS TRANSFER PROCESSES

So far, we have considered the role of stress-induced migration in altering the hydrodynamics in falling film flow of polymer solutions. Since mass transfer

involving such film flows occur quite frequently in practical situations and also mass transfer processes are controlled by the associated hydrodynamics, we feel a discussion concerning the effect of migration on such transport processes to be appropriate. Earlier, a detailed phenomenological discussion regarding the remarkable effect of wall slip in these processes have been considered by Mashelkar and Dutta [6]. They, however, used only 'heuristic' arguments to demonstrate the effect of slip and showed how the findings in the literature could be rationalized, if slip effects were incorporated. The present analysis is relatively more detailed and brings out more clearly the role of variables such as molecular weight, polymer concentration as also the flow conditions such as film thickness, angle of inclination etc. on the migration process. It needs to be emphasized that the analysis to follow will be based on FDCF asymptote and therefore it is presumed that adequate lengths would have been provided for reaching this asymptote. In the case of solid dissolution in a film (see e.g. [26]) the normal experimental arrangements provide for calming zones before the active mass transfer section starts, whereas in the case of gas absorption in a film (see e.g. [27–30]), such is not the case. The length over which macromolecular separation occurs is therefore considerably larger than the length of the mass transfer zone, whereas it is practically the same in the case of gas absorption. Further, the role of the high deformation rates in the entry region of film flows in carrying rapid separation is also uncertain. In view of these uncertainties, the analysis to follow has to be viewed with some caution.

Consider the case of mass transfer from the rigid surface (solid dissolution) and from the free surface (gas absorption) separately. In the former case, for short contact times, a Leveque-type approximation leads to the following relationship for the average mass transfer coefficient ($\bar{k}$)

$$\bar{k} \propto \left(\frac{D^2\dot{\gamma}_w}{L}\right)^{1/3} \tag{24}$$

where D is the solute diffusivity in the polymer solution, $\dot{\gamma}_w$ is the wall shear rate and L is the flow length. Since in absence of migration (no-slip case)

$$(\dot{\gamma}_w)_{ns} = \frac{2n_i+1}{n_i}\frac{q_{ns}}{\delta^2} \tag{25}$$

the ratio of mass transfer coefficient with (subscript s) and without (subscript ns) migration for a film of a given thickness becomes

$$\frac{\bar{k}_s}{\bar{k}_{ns}} = \left[-\left.\frac{d\psi}{d\xi}\right|_{\xi=1}\frac{q}{q_{ns}}\cdot\frac{n_i}{2n_i+1}\right]^{1/3} \tag{26}$$

where $d\psi/d\xi|_{\xi=1}$ is the dimensionless velocity gradient at the rigid surface in the presence of migration and the subscript i denotes evaluation at the initial polymer concentration, c_i.

In the case of mass transfer from the free surface of the film, the surface

velocity controls the convective effect and here too a penetration theory approximation, valid for short contact times, leads to the following relationship

$$\bar{k} \propto \left(\frac{D v_{max}}{L}\right)^{1/2} \tag{27}$$

where v_{max} is the maximum or the free surface velocity. As before, since

$$(v_{max})_{ns} = \frac{2n_i + 1}{n_i + 1} \frac{q_{ns}}{\delta} \tag{28}$$

the ratio of mass transfer coefficients becomes

$$\frac{\bar{k}_s}{\bar{k}_{ns}} = \left[\psi(0) \cdot \frac{q}{q_{ns}} \cdot \frac{n_i + 1}{2n_i + 1}\right]^{1/2} \tag{29}$$

where $\psi(0)$ is the dimensionless free surface velocity.

The present analysis allows determination of the wall shear rate $(d\psi/d\xi|_{\xi=1})$ and the free surface velocities $(\psi(0))$ resulting from the stress-induced migration effect. For illustrative purposes, the values for Separan MG-700 solutions considered in this work have been listed in Table II. It is seen that the (dimensionless) wall shear rate is roughly about 7–8 which is markedly higher than the corresponding no-slip values $(2 + 1/n_i \sim 4.9–5)$. Since q/q_{ns} is considerably greater than unity, Eq. (26) predicts enhanced mass transfer rates due to migration. Similarly, in the case of gas absorption even though the dimensionless surface velocity varies between 1.15–1.14, which is less than the corresponding no-slip values $(2 + 1/n_i/1 + 1/n_i \sim 1.245–1.255)$, the values of q/q_{ns} being significantly greater than unity leads to k_s/k_{ns} ratios considerably greater than unity (see Eq. (29)). These predictions are in qualitative agreement with experimental observations with such fluids, since such facilitation in dissolution rates [4, 26] and gas absorption (27–30) have been reported in the literature for falling film flows of polymer solutions.

Figure 9 illustrates the mass transfer enhancement ratio, both for transport at the rigid as well as the free surface, as a function of wall shear stress and polymer concentration for aqueous Separan MG-700 solutions. It is clearly seen that depending on the prevailing conditions the enhancement in transport rates can be anywhere between 70 to 170%. Consistently, however, the extent of augmentation is much higher for mass transfer at the free surface. Moreover, although the enhancement ratio is a monotonically increasing function of applied shear stress, the same is not true for the concentration effect. Since k_s/k_{ns} must be unity for $c_i = 0$ (i.e. water for aqueous solutions), the results depicted in Figure 9 suggest that for a given shear stress this ratio attains a maximum at some intermediate polymer concentration. Experimentally, Peev and Nikolova [4] observed that the dissolution rates of gypsum were consistently higher for 0.5% CMC solution as compared to that for 1.0% solution.

It is quite common to use the falling film technique for the measurement of diffusion coefficients. From the augmentation of mass transfer rates due to stress induced diffusion, such coefficients deduced by using ordinary hydrodynamic

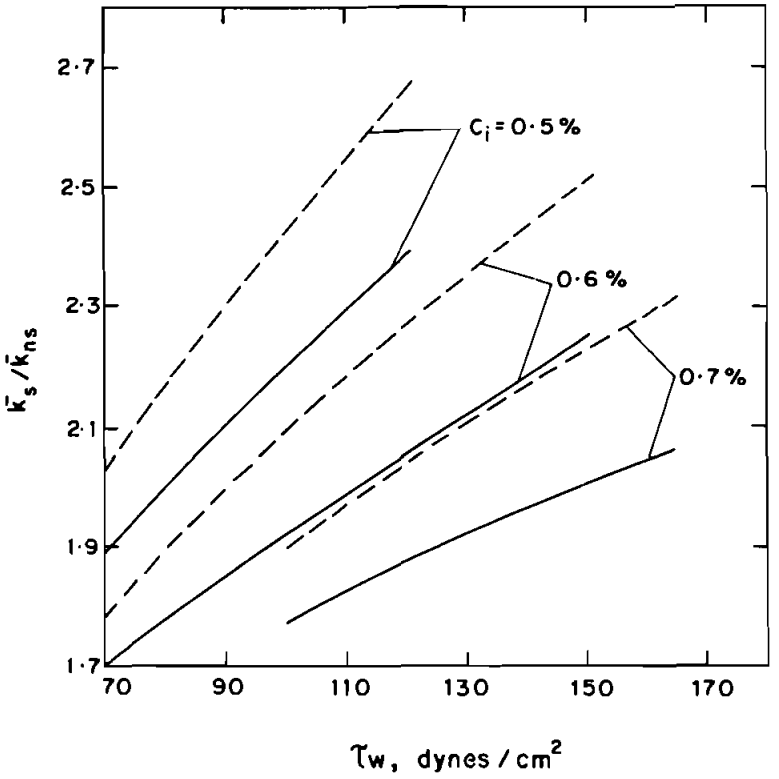

FIGURE 9 Enhancement in mass transfer rates as a function of wall shear stresss for aqueous Separan MG-700 solutions. Solid and broken lines are for mass transfer from the rigid and the free surface, respectively.

calculations can be only apparent. Further they are expected to be higher than the actual values and also should exhibit a maximum at some intermediate concentration. Indeed, such anomalous behaviour has been observed by Astarita [26] and Peev and Nikolova [4] for solid dissolution and by Perez and Sandall [27] and Mashelkar and Soylu [29, 30] for gas absorption. It, therefore, appears that the falling film technique may not be reliable, since erroneous results may be obtained due to stress induced migration effects.

REFERENCES

1. Popadic, V.O., *AIChE. J.*, **21,** 610 (1975).
2. Astarita, G., Marrucci, G., and Palumbo, G., *Ind. Eng. Chem. Fundam.*, **3,** 333 (1964).
3. Carreau, P.J., Bui, Q.H., and Leroux, P., *Reol. Acta*, **18,** 600 (1979).
4. Peev, G., and Nikolova, A., *J. Non-Newt. Fluid Mech.*, **8,** 319 (1981).
5. Dutta, A., and Mashelkar, R.A., *AIChE. J.*, **29,** 519 (1983).
6. Mashelkar, R.A., and Dutta, A., *Chem. Eng. Sci.*, **37,** 969 (1982).
7. Metzner, A.B., Cohen, Y., and Rangel-Nafaile, C., *J. Non-Newt. Fluid Mech.*, **5,** 449 (1979).
8. Tirrell, M., and Malone, M.F., *J. Polym. Sci., Polym. Phys. Ed.*, **15,** 1569 (1977).
9. Aubert, J.H., and Tirrell, M., *J. Chem. Phys.*, **77,** 533 (1982).
10. Brunn, P.O., *J. Chem. Phys.*, **80,** 5821 (1984).

11. Janssen, L.P.B.M., *Reol. Acta*, **19,** 32 (1980).
12. Dutta, A., and Mashelkar, R.A., *J. Non-Newt. Fluid Mech.*, **16,** 279 (1984).
13. Cohen, Y., and Metzner, A.B., *AIChE. Symp. Ser.*, **212, 78,** 77 (1982).
14. Cohen, Y., Ph.D. Thesis, University of Delaware, Newark, Delaware, 1980.
15. Dutta, A., and Mashelkar, R.A., *Rheol. Acta*, **22,** 455 (1983).
16. Peterlin, A., *Pure Appl. Chem.*, **12,** 563 (1966).
17. Separan Polymers Brochure, Dow Chemical Co., Midland, Michigan, 1981.
18. Abdel-Khalik, S.I., Hassager O., and Bird, R.B., *Polym. Eng. Sci.*, **14,** 859 (1972).
19. Wagner, M.H., *Rheol. Acta*, **16,** 43 (1977).
20. Gordon, R.J., and Schowlater, W.R., *Trans. Soc. Rheol.*, **16,** 79 (1972).
21. Kulicke, W.M., Kniewske, R., and Klein, J., *Progr. Polym. Sci.*, **18,** 373 (1982).
22. Argumedo, A., Chung, T.T., and Chang, K.I., *J. Rheol.*, **22,** 449 (1978).
23. Vrentas, J.S., and Duda, J.L., *AIChE. J.*, **25,** 1 (1979).
24. Scholtan, W., *Makromol. Chemie*, **14,** 169 (1954).
25. Dutta, A., and Mashelkar, R.A., *Rheol. Acta*, **21,** 52 (1982).
26. Astarita, G., *Ind. Eng. Chem. Fund.*, **5,** 14 (1965).
27. Perez, J.F., and Sandall, O.C., *AIChE. J.*, **19,** 1073 (1973).
28. Mashelkar, R.A., *AIChE. J.*, **30,** 353 (1984).
29. Mashelkar, R.A., and Soylu, M., *Chem. Eng. Sci.*, **29,** 1089 (1974).
30. Mashelkar, R.A., and Soylu, M., *J. Appl. Polym. Sci.*, **27,** 697 (1982).